

Multistability of carbon nanotube packings on flat substrate

A. V. Savin^{1,2,*}

¹ *N.N. Semenov Federal Research Center for Chemical Physics,
Russian Academy of Sciences (FRCCP RAS), Moscow, 119991, Russia*

² *Plekhanov Russian University of Economics, Moscow, 117997 Russia*

It is shown by the method of molecular dynamics using a chain model that a multilayer packaging of identical single-walled carbon nanotubes with a diameter of $D > 2.5$ nm located on a flat substrate is a multistable system. The system has many stationary states, which are characterized by the portion of collapsed nanotubes. The thickness of the package monotonically decreases with an increase in the portion of such nanotubes. For nanotubes with a chirality index (60,0), depending on the portion of collapsed nanotubes, the thickness of the 11-layer package can vary from 12 to 36 nm. All stationary states of the package are stable to thermal fluctuations at $T = 300$ K. The transverse compression of the package is not elastic; due to the collapse of a part of the nanotubes, it only transfers the package from one stationary state to another with a smaller thickness.

I. INTRODUCTION

Carbon nanotubes (CNTs) are macromolecules with a cylindrical form with a diameter starting from 0.4 nm and lengths up to few microns. Similar structures were detected for the first time during the thermal decomposition of carbon monoxide on an iron contact [1]. CNTs as such were obtained considerably later as side products of C₆₀ fullerene synthesis [2]. Currently, CNTs attract interest due to their unique properties [3]. CNTs with desired geometric properties (i.e., with the required diameter, length, and chirality) can be readily synthesized [4, 5] and used to prepare bundles of parallel CNTs [6, 7]. Such materials, also referred to as CNT forests or arrays, feature even more superior mechanical properties, compared to isolated CNTs, due to van der Waals interactions between them [8].

A number of computational approaches have been developed for the study of structures based on CNTs in addition to the well-known molecular dynamics method. Deformation mechanisms of CNT forest have been studied using mesoscopic modeling in [9, 10]. A continuum thin shell theory is capable of describing large deformations of CNTs [11]. Mechanical properties of CNTs under transverse loading have been studied in [12]. In the review [13] the power of the nonlocal beam, plate, and shell theories in modeling mechanical properties of nanomaterials is described. The application of the continuum beam theory has been demonstrated in [14]. Simulation of the mechanical properties and failure of the CNT bundles have been performed using a nonlinear coarse-grained stretching and bending potentials [15].

CNTs of a diameter greater than a threshold value can exist in circular and in collapsed forms due to the competition between CNT wall bending and van der Waals interactions [16–20]. Unlike dense materials, CNT crystal

can demonstrate very high compressibility in the elastic region. Practically, CNT bundles can be used, e.g., for protection against shocks and vibrations [21, 22].

In this work, we consider CNT arrays on a flat substrate formed by the surface of hexagonal boron nitride (h-BN) crystal. Using chain model offered in [23] and modified for the CNT bundle in [24], we will show that the multilayer packaging of single-walled nanotubes on a flat substrate is a multistable system. The stationary states of the packages differ slightly in energy, but they can differ several times in thickness.

II. THE MODEL

An array (a bundle) of CNTs can be conveniently described with a 2D model of a system of cyclic molecular chains [23, 25]. For a single-walled CNT with a zigzag structure (with chirality index $(m, 0)$), the chain model describes the nanotube's transversal cross section that forms a ring-shaped chain of $N = 2m$ effective particles corresponding to longitudinal lines of atoms in the nanotube.

Under plane strain conditions, the cross section of a CNT completely determines its deformed state. Then a bundle of defect-free CNTs can be represented by a set of their cross sections, which significantly reduces the number of considered degrees of freedom. This model was previously successfully used in modeling the scrolls of graphene nanoribbons [23], windings of nanoribbons around CNTs [25], analysis of mechanical properties of CNT bundle upon uniaxial and biaxial lateral compression [24].

For definiteness, a bundle of straight, single-walled zigzag CNTs with chirality $(m, 0)$ oriented along the z -axis of the Cartesian coordinate system, as shown in Fig. 1, is considered. The cross sections of such CNT contain $N = 2m$ carbon atoms, each of which represents a straight chain of atoms normal to the (x, y) -plane. Each atom in the cross section of a CNT has two degrees of

*Electronic address: asavin@center.chph.ras.ru

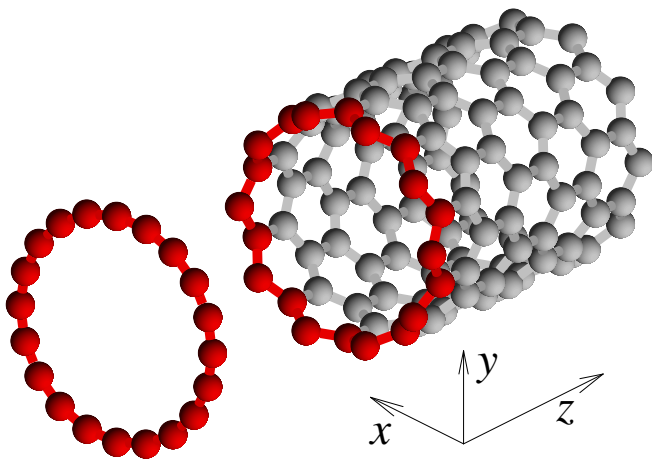


FIG. 1: A scheme for constructing a 2D chain model of single-walled zigzag carbon nanotube. Nanotube with chirality index of $(m, 0)$ with $m = 10$ and corresponding cross section of $N = 2m$ carbon atom is shown.

freedom, namely, coordinates on the (x, y) -plane.

The Hamiltonian for single CNT cross section, with the atoms numbered by the index $n = 1, \dots, N$, can be written in the form

$$H = \sum_{n=1}^N \left[\frac{1}{2} M (\dot{\mathbf{u}}_n, \dot{\mathbf{u}}_n) + V(R_n) + U(\theta_n) + W_0(y_n) + \frac{1}{2} \sum_{\substack{l=1 \\ |l-n|>4}}^N W_1(r_{nk}) \right], \quad (1)$$

where the 2D vector $\mathbf{u}_n = (x_n, y_n)$ defines the coordinates of the n -th particle in the cycle chain, and $M = 12m_p$ is the carbon atom mass ($m_p = 1.6603 \cdot 10^{-27}$ kg is the proton mass).

The potential

$$V(R) = \frac{1}{2} K (R - R_0)^2, \quad (2)$$

describes the longitudinal chain stiffness, where K is the interaction stiffness, R_0 is the equilibrium bond length (chain period), and $R_n = |\mathbf{v}_n|$ is the distance between adjacent n and $n+1$ nodes (vector $\mathbf{v}_n = \mathbf{u}_{n+1} - \mathbf{u}_n$).

The potential

$$U(\theta) = \epsilon_\theta [1 + \cos(\theta)], \quad (3)$$

describes the bending stiffness of the chain, where θ is the angle between two adjacent bonds, cosine of the n -th valence angle $\cos(\theta_n) = -(\mathbf{v}_{n-1}, \mathbf{v}_n) / R_{n-1} R_n$.

The parameters of potentials (2) and (3) were determined in [23] by analyzing dispersion curves for a graphene nanoribbon: longitudinal stiffness $K = 405$ N/m, chain period $R_0 = r_c \sqrt{3}/2$ (where $r_c = 1.418$ Å is the length of C-C valence bond in the

graphene sheet, $R_0 = 1.228$ Å), and energy $\epsilon_\theta = 3.5$ eV. The diameter of an isolated $(m, 0)$ nanotube is $D = R_0 / \sin(\pi/2m) \approx 2mR_0/\pi$.

Potential $W(r_{n,k})$ describes weak non-covalent interactions between remote nodes n and k of the chain, where $r_{n,k} = |\mathbf{u}_k - \mathbf{u}_n|$ is the distance between the nodes. This potential was also used to describe the interaction between nodes of different chains (different nanotubes). The potential of non-covalent interaction between chain nodes can be described with high accuracy [26] by the (5,11) Lennard-Jones potential

$$W_1(r) = \epsilon_1 [5(r_0/r)^{11} - 11(r_0/r)^5] / 6, \quad (4)$$

with equilibrium bond length $r_0 = 3.607$ Å and interaction energy $\epsilon_1 = 0.00832$ eV.

In the chain Hamiltonian (1), potential $W_0(y)$ describes the interaction between a chain node and the substrate formed by the flat surface of a molecular crystal. In modeling, we take that the substrate surface coincides with the plane $y = 0$. To determine this potential, we established numerically the dependence of the energy of interaction between a carbon atom and the substrate on its distance to the surface plane y . Calculations [26, 27] showed that the energy $W_0(y)$ of interaction with the substrate can be described with good accuracy by the (k, l) Lennard-Jones potential:

$$W_0(h) = \epsilon_0 [k(h_0/h)^l - l(h_0/h)^k] / (l - k), \quad (5)$$

where $l > k$. Potential (5) has the minimum $W_0(h_0) = -\epsilon_0$, where ϵ_0 is the energy of bonding between a carbon atom and a substrate, and h_0 is the equilibrium distance from the surface plane of the substrate. Potential (5) allows us to describe the interaction of a carbon atom with flat surfaces of molecular crystals of ice I_h , graphite, silicon carbide $6H$ -SiC, silicon and silver [27]. We will use the flat surface of hexagonal boron nitride (h-BN) as a substrate, since it is the ideal substrate for graphene nanoribbon and nanotube [28, 29]. For the h-BN surface interaction energy is $\epsilon_0 = 0.0903$ eV, the equilibrium distance is $h_0 = 3.46$ Å, and the exponents are $l = 10$ and $k = 3.75$.

The potentials (4) and (5) are obtained as the sums of the Lennard-Jones potentials (6,12) describing the Van der Waals interactions of pairs of atoms. Therefore, in 2D model they describe Van der Waals interactions. The bending stiffness of nanotubes is described by the potentials (2) and (3). Due to the isotropy of the stiffness of the graphene sheet, all results obtained for nanotubes with the chirality index $(m, 0)$ will be valid for all other types of nanotubes with the same diameter D .

III. STEADY STATES OF TWO INTERACTION NANOTUBES

Nanotubes exhibit a high longitudinal (axial) and relatively low transverse (radial) stiffness. Because of this,

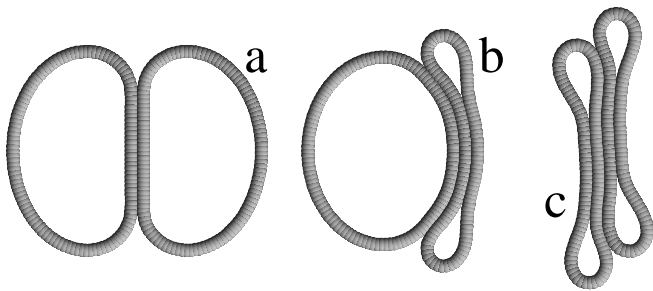


FIG. 2: The stationary states of two interacting isolated nanotubes (60,0) (the number of chain nodes $N = 120$): (a) open, (b) open and collapsed, (c) collapsed nanotubes. State energies $E = -1.021, -1.223, -0.740$ eV, nanotube cross-sectional areas $S = 30.84, 20.52, 7.72$ nm².

a nanotube with a quite large diameter can undergo the transition from a hollow cylindrical shape to a collapsed state [16, 30–32] due to the nonvalent interaction of its layers. Let us consider the possible stationary states of a system of two interacting nanotubes.

Let the node coordinates of the k -th nanotube (k -th cyclic chain) with chirality index $(m, 0)$ be defined by $2N$ -dimensional vector $\mathbf{x}_k = \{\mathbf{u}_{k,n}\}_{n=1}^N$, where $N = 2m$ and $k = 1, 2$. Then, the energy of nanotube deformation is

$$P_1(\mathbf{x}_k) = \sum_{n=1}^N [V(R_n) + U(\theta_n) + W_0(y_n) + \frac{1}{2} \sum_{\substack{l=1 \\ |l-n|>4}}^N W_1(r_{n,l})]. \quad (6)$$

The potential energy of nanotube system is

$$E = P_1(\mathbf{x}_1) + P_1(\mathbf{x}_2) + P_2(\mathbf{x}_1, \mathbf{x}_2), \quad (7)$$

where the function

$$P_2(\mathbf{x}_1, \mathbf{x}_2) = \sum_{n_1=1}^N \sum_{n_2=1}^N W_1(r_{1,n_1;2,n_2})$$

determines the energy of interaction between cyclic chains, $r_{1,n_1;2,n_2} = |\mathbf{u}_{1,n_1} - \mathbf{u}_{2,n_2}| = [(x_{2,n_2} - x_{1,n_1})^2 + (y_{2,n_2} - y_{1,n_1})^2]^{1/2}$ is the distance between chain nodes.

To find the steady state of the CNT system, we must solve the energy minimization problem:

$$E \rightarrow \min : \{\mathbf{x}_k\}_{k=1}^2. \quad (8)$$

Minimization problem (8) was solved numerically by a conjugated gradient method. The stationary state of system of 2 CNTs $\{\mathbf{x}_k^0\}_{k=1}^2$ is characterized by the energy E and by the cross-sectional area of the nanotubes S .

A characteristic picture of the three possible stationary states is shown in Fig. 2. Two CNTs with a chirality index (60,0) (the number of atoms in each chain $N = 120$) have three stationary stable states: (a) the state in which each nanotube is in the open state, energy $E =$

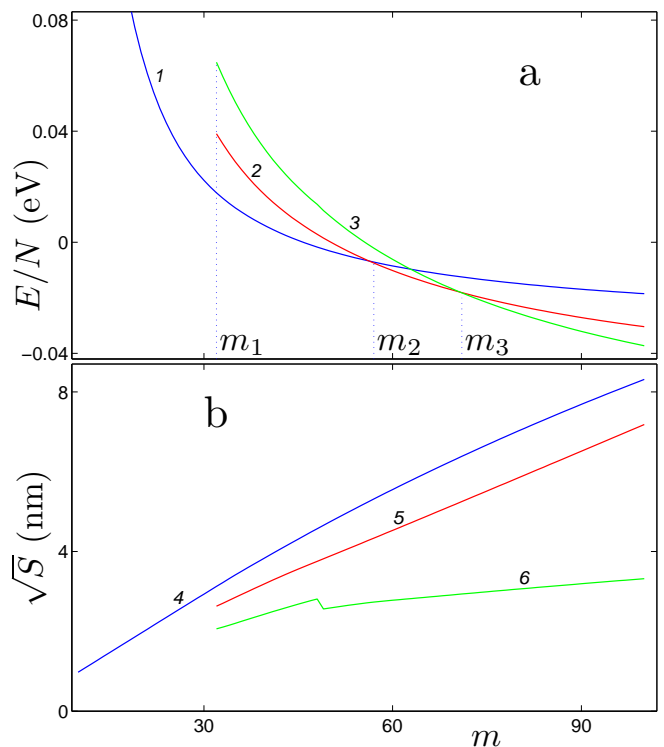


FIG. 3: The dependence of (a) the energy E/N and of (b) the square root of the cross-sectional area \sqrt{S} of two interacting isolated nanotubes on the value of their chirality index $(m, 0)$ (curves 1, 4 for open; 2, 5 for open and collapsed, and 3, 6 for collapsed nanotubes, $N = 2m$). The characteristic values of the index are $m_1 = 32, m_2 = 57, m_3 = 71$.

-1.021 , cross-sectional area $S = 30.84$; (b) one nanotube is in the open and the other in the collapsed state, $E = -1.223$, $S = 20.52$; (c) all nanotubes are in a collapsed state $E = -0.740$ eV, $S = 7.72$ nm².

The dependence of the energy E and the cross-sectional area S of two interacting nanotubes on the value of their chirality index $(m, 0)$ is shown in Fig. 3. The solution of the minimum problem (8) has demonstrated that at $m < 32$ there is only one stationary state in which all nanotubes are in the open state. At $m \geq 32$, the system of two nanotubes already has three stationary states: the state of open CNTs, the state of open and collapsed CNTs, and the state of collapsed CNTs – see Fig. 2. All states are stable. At the index $m < 57$, the main state, i.e. the state with minimal energy, is the state of open CNTs, at $57 \leq m < 71$ – the state of open and collapsed CNTs, at $m \geq 71$ – the state of collapsed CNTs. Therefore, it should be expected that nanotube systems with a chirality index of $(m, 0)$ at $m > 32$ (with diameter $D > 2.5$ nm) will have many stationary states, which will be characterized by the portion of collapsed nanotubes.

If interacting nanotubes are on a flat substrate, then six stationary stable states of two nanotubes are already possible – see Fig. 4. They differ from each other not only

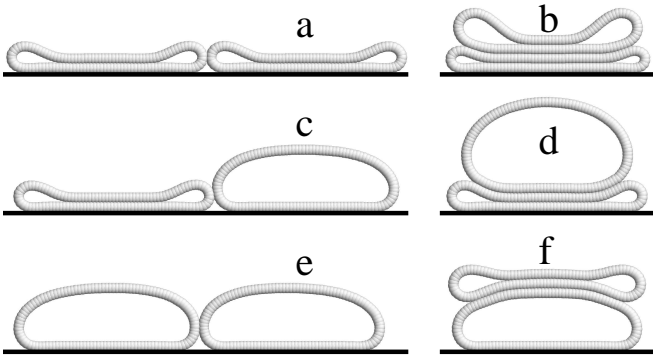


FIG. 4: The stationary states of two interacting nanotubes (60,0) (the number of chain nodes $N = 120$) located on a flat substrate: (a) collapsed (longitudinal), (b) collapsed (vertical), (c) collapsed and open (longitudinal), (d) collapsed and open (vertical), (e) open (longitudinal), (f) open and collapsed (vertical arrangement). State energies $E = -8.634, -5.970, -8.009, -6.384, -7.409, -4.987$ eV, nanotube cross-sectional areas $S = 6.36, 7.15, 14.52, 18.03, 22.90, 14.31$ nm². Horizontal lines show the plane of the substrate.

in the open or closed (collapsed) state of the nanotubes but also in their mutual position relative to the substrate plane. Thus, each nanotube can lie on the substrate, forming longitudinal arrangements (a), (c) and (e), or lie on top of each other, forming vertical arrangements (b), (d) and (f) in which only one of them is in contact with the substrate.

The dependence of the energy E and the cross-sectional area S of two interacting nanotubes located on a flat substrate on the value of their chirality index $(m, 0)$ is shown in Fig 5. The solution of the minimum problem (8) has demonstrated that the longitudinal arrangement of nanotubes on the substrate plane is always more energetically advantageous. At $m < 49$, the most advantageous state is the longitudinal arrangement of open nanotubes, at $m > 49$ – the longitudinal arrangement of closed nanotubes.

IV. MULTILAYER NANOTUBE PACKING

Let us analyze the conformational changes of multilayer packages of single-walled nanotubes during their transverse compression. We consider a system of parallel $N_{xy} = N_x \times N_y$ nanotubes $(m, 0)$ located between two flat substrates (N_x is the number of nanotubes in one layer parallel to the substrate, N_y is the number of layers) – see Fig. 6(a). Along the x axis, we will use periodic boundary conditions with the period a_x .

The node coordinates of the k -th nanotube (k -th cyclic chain) are defined by $2N$ -dimensional vector $\mathbf{x}_k = \{\mathbf{u}_{k,n}\}_{n=1}^N$, $N = 2m$, $k = 1, \dots, N_{xy}$. The energy of the

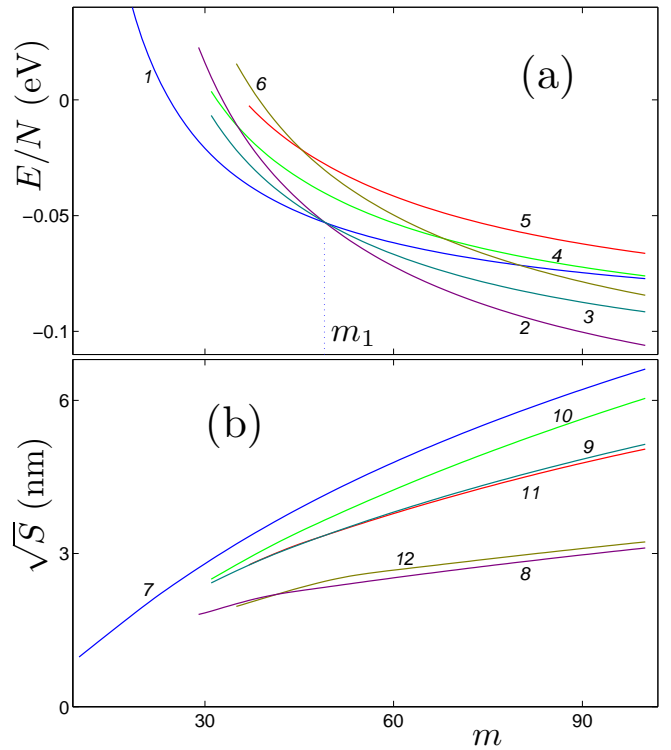


FIG. 5: The dependence of (a) the energy E/N and of (b) the square root of the cross-sectional area \sqrt{S} of two interacting nanotubes located on a flat substrate on the value of their chirality index $(m, 0)$ (curves 1, 7 for open (longitudinal); 2, 8 for collapsed (longitudinal); 3, 9 for collapsed and open (longitudinal); 4, 10 for collapsed and open (vertical); 5, 11 for open and collapsed (vertical), and 6, 12 for collapsed nanotubes (vertical arrangement), $N = 2m$). The characteristic value of the index is $m_1 = 49$.

nanotube deformation has the form

$$P_1(\mathbf{x}_k) = \sum_{n=1}^N [V(R_n) + U(\theta_n) + W_0(y_{k,n}) + W_0(h - y_{k,n}) + \frac{1}{2} \sum_{\substack{l=1 \\ |l-n|>4}}^N W_1(r_{n,l})], \quad (9)$$

where h is distance between the surfaces of flat substrates. The potential energy of nanotube packing per unit cell (per period) is

$$E = \sum_{k=1}^{N_{xy}} P_1(\mathbf{x}_k) + \sum_{k_1=1}^{N_{xy}-1} \sum_{k_2=k_1+1}^{N_{xy}-1} [P_2(\mathbf{x}_{k_1}, \mathbf{x}_{k_2}) + P_2(\mathbf{x}_{k_1}, \mathbf{x}_{k_2} + a_x \mathbf{e}_x)], \quad (10)$$

where vector $\mathbf{e}_x = \{(1, 0)\}_{n=1}^N$.

Let us take for certainty the index $m = 60$ (the number of nodes in the chain $N = 120$), the number of nanotube layers $N_y = 11$, the number of nanotubes in one layer $N_x = 18$, the unit cell size (period) $a_x = 94.9$ nm. The

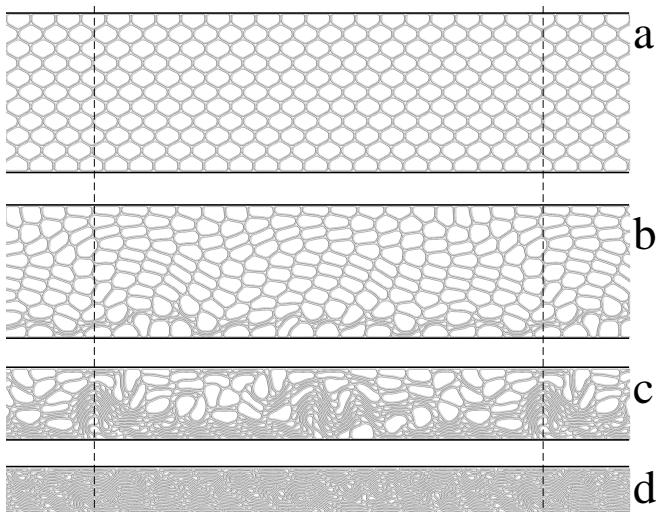


FIG. 6: The picture of stationary states of a layered structure consisting of $N_x \times N_y$ nanotubes (60,0) (the number of nanotubes in one layer $N_x = 18$, the number of layers $N_y = 11$, the number of atoms in each cyclic chain $N = 120$) on a distance h between the compressive planes: (a) $h = 36$ (state energy $E = -384.08$, pressure on the plane $P = 0.00012$); (b) $h = 30$ ($E = -378.49$, $P = 0.00042$); (c) $h = 16$ ($E = -352.16$, $P = 0.00084$); (d) $h = 10$ nm ($E = -229.35$ eV, $P = 0.01156$ eV/Å³). Horizontal lines show the compressive planes, while vertical lines show the boundaries of the periodic cell (period $a_x = 94.9$ nm).

stationary state of a multilayer system of nanotubes was found numerically as a solution to the minimum energy problem

$$E \rightarrow \min : \{\mathbf{x}_k\}_{k=1}^{N_{xy}} \quad (11)$$

for fixed values of the distance between the layers h and the unit cell size a_x .

Let us first take $h = 36.8$ nm and get the stationary state of the multilayer packaging of open nanotubes – see Fig. 6. Then we will gradually reduce the distance between the layers h . Compression will lead to the collapse of a part of the nanotubes. The number of collapsed nanotubes increases monotonically with a decrease in the distance between the layers. At $h = 10.9$ nm, almost all nanotubes will already be in the collapsed state.

Each stationary state $\{\mathbf{x}_k^0\}_{k=1}^{N_{xy}}$ is characterized by the energy E and by the pressure on the substrate plane

$$P = \frac{1}{3a_x r_c} \sum_{k=1}^{N_{xy}} [W'_0(h - y_{k,n}^0) - W'_0(y_{k,n}^0)].$$

The dependence of E and P on h is shown in Fig. 7. As can be seen from the figure, the range of values of h can be divided into three zones. At $h > h_2 = 36$ nm, the walls stretch a multilayer system of open nanotubes. The compression of the nanotube system begins to occur

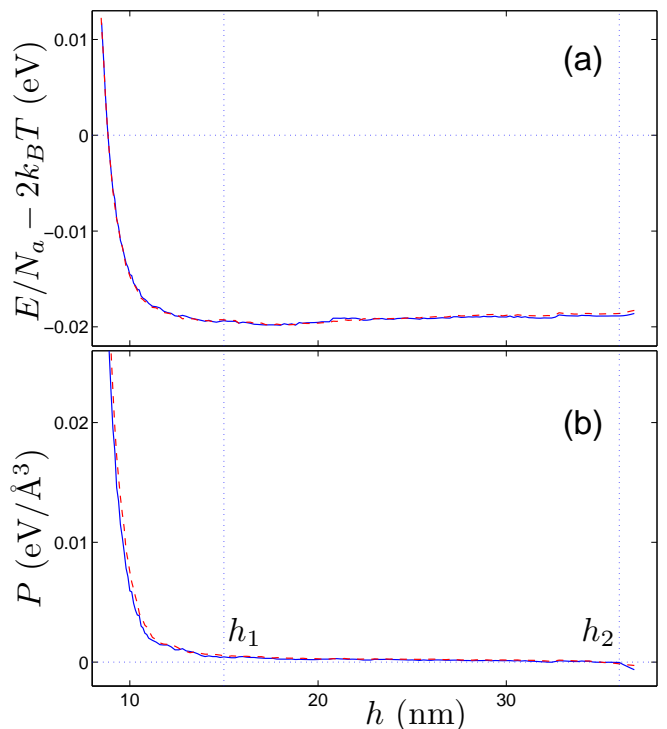


FIG. 7: The dependence of (a) the energy E normalized by the total number of atoms of the system $N_a = N_x N_y N$ and (b) the pressure P on the distance between the compressive planes h . The characteristic values are $h_1 = 15$, $h_2 = 36$ nm. The solid (blue) curves show the dependence for the states of the CNT system at a temperature of $T = 0$, the dotted (red) curves – at $T = 300$ K.

only when the distance between the layers $h < h_2$. In the range of values $h_1 < h < h_2$, $h_1 = 15$, compression leads only to a decrease in the energy of the system E and to a weak linear increase in pressure P . The energy and the pressure begin to increase sharply at $h < h_1$. The minimum energy is achieved when the compression $h = 17.4$ nm.

In order to obtain the free state of the multilayer packaging of nanotubes, we will remove one substrate and solve the minimum problem (11) using the compressed stationary state as the starting point in the conjugate gradient method. As a result, we get a stationary state of the multilayer packaging of nanotubes $\{\mathbf{x}_k^0\}_{k=1}^{N_{xy}}$ at zero pressure. Each such state will be characterized by the energy E and by the average thickness of the packaging

$$h_y = \frac{2}{N_a} \sum_{k=1}^{N_{xy}} \sum_{n=1}^N y_{k,n}^0,$$

where the total number of atoms of CNT system $N_a = N_{xy} N = N_x N_y N$.

A characteristic view of stationary uncompressed multilayer nanotube packages is shown in Fig. 8. Calculations have shown that the multilayer system of nanotubes

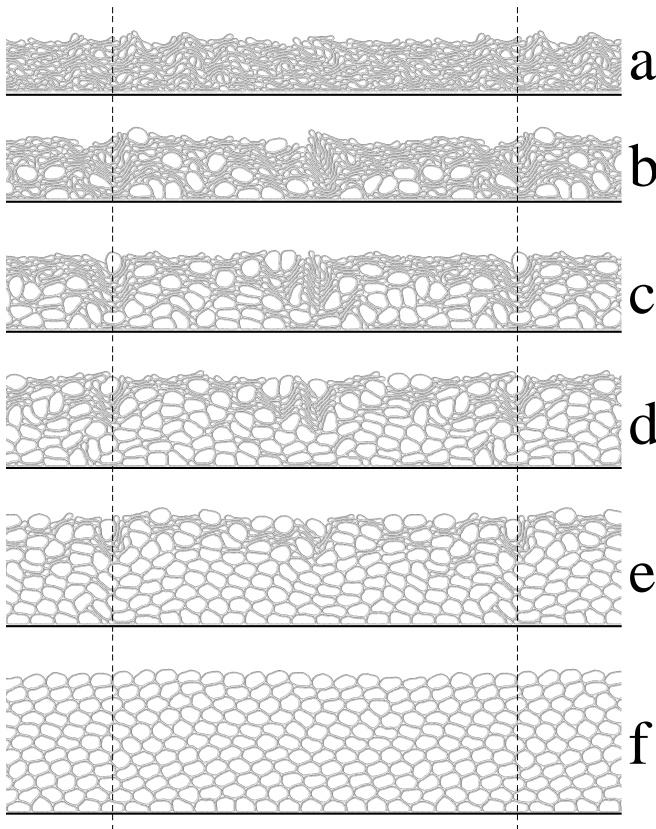


FIG. 8: The picture of stable states of layered structures consisting of $N_x \times N_y$ nanotubes (60,0) (the number of nanotubes in one layer $N_x = 18$, the number of layers $N_y = 11$, the number of atoms in each cyclic chain $N = 120$) located on a flat substrate with an average thickness of the structure (a) $h_y = 12.98$, (b) 16.14, (c) 20.49, (d) 24.90, (e) 30.14, (f) 35.10 nm. The states are shown at a temperature of $T = 300$ K. Horizontal lines show the plane of the substrate, while vertical lines – the boundaries of the periodic cell (period $a_x = 94.9$ nm).

(60,0) is a multistable, its stationary states can have an average thickness of $12 < h_y < 36$ nm – see Fig. 9. Thus, the thickness of different packages may differ by three times. All stationary packages are stable to thermal fluctuations and differ in the ratio of the number of open to the number of collapsed nanotubes (the more is the number of open nanotubes, the greater is the package thickness). The thickest is the package with all open nanotubes (see Fig. 8f), its thickness is $h_y = 35.10$ nm, the thinnest is the package with all collapsed nanotubes (see Fig. 8a), its thickness is $h_y = 12.98$ nm.

The dependence of the energy of N_y -layer packages on their thickness is shown in Fig. 9. As can be seen from the figure, the energy of the packages weakly depends on their thickness. The minimum energy $E/N_a = -0.017$ eV is achieved at thickness $h_y = 20$ nm.

Note that all the stationary states of nanotube arrays obtained using the 2D model will correspond to the sta-

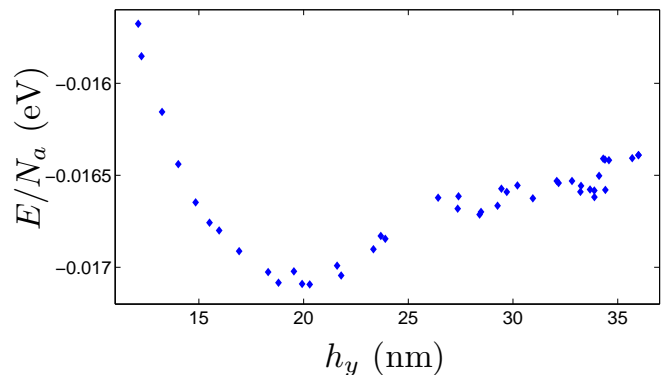


FIG. 9: The dependence of the energy of stationary states of layered structures consisting of $N_x \times N_y$ nanotubes (60,0) (the number of nanotubes in one layer $N_x = 18$, the number of layers $N_y = 11$, the number of atoms in each cyclic chain $N = 120$) located on a flat substrate on the average thickness of the structure h_y .

tionary states in the 3D model if the lengths of the nanotubes significantly exceed their diameters (if $L \gg D$).

V. ACCOUNTING OF THERMAL VIBRATIONS

To check the stability of the stationary states of multilayer nanotube packages, molecular dynamic modeling was performed at a temperature of $T = 300$ K. A system of Langevin equations was numerically integrated to simulate thermal oscillations

$$M\ddot{\mathbf{x}}_k = -\frac{\partial E}{\partial \mathbf{x}_k} - \Gamma M \dot{\mathbf{x}}_k - \Xi_k, \quad k = 1, \dots, N_{xy}, \quad (12)$$

where \mathbf{x}_k is $2N$ -dimensional vector giving the coordinates of the k th nanotube, E is potential energy of molecular system (10), M is the mass of carbon atom, Γ is the friction coefficient (the relaxation time $t_r = 1/\Gamma$ is 1 ps), $\Xi_k = \{(\xi_{k,n,1}, \xi_{k,n,2})\}_{n=1}^N$ is $2N$ -dimensional vector of normally distributed random Langevin forces with the following correlations:

$$\langle \xi_{k_1, n_1, i}(t_1) \xi_{k_2, n_2, j}(t_2) \rangle = 2Mk_B T \Gamma \delta_{k_1 k_2} \delta_{n_1 n_2} \delta_{ij} \delta((t_2 - t_1))$$

(k_B is Boltzmann constant, T is temperature of the Langevin thermostat).

As an initial condition for the equations of motion (12) we take the stationary state of nanotube packaging. Numerical integration of the system of equations of motion (12) showed that all stationary states of the nanotube system are stable to thermal fluctuations. As can be seen from Fig. 7, thermal fluctuations not lead to a significant change in the type of dependencies $E(h)$ and $P(h)$.

VI. NUMERICAL METHODS

The minimum energy problems (8), (11) were solved

numerically by the conjugate gradient method [33]. The system of equations of motion (12) was integrated numerically using the velocity form of the Verlet difference scheme [34]. All the simulation programs were written in FORTRAN. Programs RasMol and RasTop were used for the visualization of obtained results. The main calculations were carried out on supercomputers of the Joint Supercomputer Center, Russian Academy of Sciences.

VII. CONCLUSIONS

The simulation has shown that the multilayer packaging of identical single-walled nanotubes with a diameter $D > 2.5$ nm located on a flat substrate is a multistable system. The system has many stationary states, which are characterized by the portion of collapsed nanotubes. The thickness of the package monotonically decreases with an increase in the portion of such nanotubes. For nanotubes with a chirality index (60,0), the thickness of the 11-layer package can vary from 12 to 36 nm, depending on the portion of collapsed nanotubes. All stationary

states of the package are stable to thermal fluctuations at $T = 300$ K. The transverse compression of the package is not elastic, it only, due to the collapse of a part of the nanotubes, transfers the package from one stationary state to another with a smaller width.

Compression of CNT packages will occur elastically only for $(m, 0)$ nanotubes with the index $m \leq 32$ (for CNT with diameter $D \leq 2.5$ nm). If we take any strongly compressed stationary state of a multilayer package and allow free movement of the compressing walls, the package will expand and return to its basic uncompressed state. Such multi-layer packages will give the best protection against vibrations.

Acknowledgements

The work was supported by the Russian Foundation for Basic Research and by the Department of Science and Technology, Ministry of Science and Technology, Government of India, within scientific project no. 19-58-45036. Computational resources were provided by the Joint Supercomputer Center, Russian Academy of Sciences.

-
- [1] L. V. Radushkevich and V. M. Luk'yanovich, The Structure of Carbon Forming in Thermal Decomposition of Carbon Monoxide on an Iron Catalyst. *Russian Journal of Physical Chemistry*, **26**, 88-95. (In Russian).
- [2] S. Iijima, Synthesis of Carbon Nanotubes. *Nature (London, U.K.)* **354**, 56-58 (1991).
- [3] D. Qian, G.J. Wagner, W.K. Liu, M.-F. Yu, R.S. Ruoff, Mechanics of carbon nanotubes. *Appl. Mech. Rev.* **55**, 495-532 (2002).
- [4] J. Di, S. Fang, F. A. Moura, D. S. Galvao, J. Bykova, A. Aliev, M. J. d. Andrade, X. Lepro, N. Li, C. Haines, R. Ovalle-Robles, D. Qian and R. H. Baughman, Strong, Twist-Stable Carbon Nanotube Yarns and Muscles by Tension Annealing at Extreme Temperatures. *Advanced Materials* **28**, 6598-6605 (2016).
- [5] Y. Bai, R. Zhang, X. Ye, Z. Zhu, H. Xie, B. Shen, D. Cai, B. Liu, C. Zhang, Z. Jia, S. Zhang, X. Li and F. Wei, Carbon nanotube bundles with tensile strength over 80 GPa. *Nature Nanotechnology* **13**, 589-595 (2018).
- [6] B.C. Liu, T.J. Lee, S.H. Lee, C.Y. Park, and C.J. Lee, Large-scale synthesis of high-purity well-aligned carbon nanotubes using pyrolysis of iron(II) phthalocyanine and acetylene. *Chemical Physics Letters* **377**, 55-59 (2003).
- [7] Y. Li, X. Zhang, X. Tao, J. Xu, W. Huang, J. Luo, Z. Luo, T. Li, F. Liu, Y. Bao, and H.J. Geise, Mass production of high-quality multi-walled carbon nanotube bundles on a Ni/Mo/MgO catalyst. *Carbon* **43**, 2, 295-301 (2005).
- [8] E.G. Rakov, Carbon nanotubes in new materials. *Russ. Chem. Rev.* **82** (1), 27-47 (2013).
- [9] B.K. Wittmaack, A.N. Volkov, L.V. Zhigilei, Mesoscopic modeling of the uniaxial compression and recovery of vertically aligned carbon. *Compos. Sci. Technol.* **166**, 66-85 (2018).
- [10] B.K. Wittmaack, A.N. Volkov, L.V. Zhigilei, Phase transformation as the mechanism of mechanical deformation of vertically aligned carbon nanotube arrays: Insights from mesoscopic modeling. *Carbon* **143**, 587-597 (2019).
- [11] B.I. Yakobson, C.J. Brabec, J. Bernholc, Nanomechanics of carbon tubes: Instabilities beyond linear response. *Phys. Rev. Lett.* **76**, 2511-2514 (1996).
- [12] E. Saether, S.J.V. Frankland, R.B. Pipes, Transverse mechanical properties of single-walled carbon nanotube crystals. Part I: Determination of elastic moduli. *Compos. Sci. Technol.* **63**, 1543-1550 (2003).
- [13] H. Rafii-Tabar, E. Ghavanloo, S.A. Fazelzadeh, Nonlocal continuum-based modeling of mechanical characteristics of nanoscopic structures. *Phys. Rep.* **638**, 1-97 (2016).
- [14] V.M. Harik, Ranges of applicability for the continuum beam model in the mechanics of carbon nanotubes and nanorods. *Solid State Commun.* **120**, 331-335 (2001).
- [15] J. Ji, J. Zhao, W. Guo, Novel nonlinear coarse-grained potentials of carbon nanotubes. *J. Mech. Phys. Solids* **128**, 79-104 (2019).
- [16] N. S. Chopra, L. X. Benedict, V. H. Crespi, M. L. Cohen, S. G. Louie, and A. Zettl, Fully collapsed carbon nanotubes. *Nature (London, U.K.)* **377**, 135-138 (1995).
- [17] T. Chang, Dominoes in carbon nanotubes. *Phys. Rev. Lett.* **101**, 175501 (2008).
- [18] A. Impellizzeri, P. Briddon, C.P. Ewels, Stacking- and chirality-dependent collapse of single-walled carbon nanotubes: A large-scale density-functional study. *Phys. Rev. B* **100**, 115410 (2019).
- [19] J. Cui, J. Zhang, X. Wang, B. Theogene, W. Wang, H. Tohmyoh, X. He, and X. Mei, Atomic-Scale Simulation of the Contact Behavior and Mechanism of the SWNT-AgNW Heterostructure. *J. Phys. Chem. C* **123**(32), 19693-19703 (2019).
- [20] M.M. Maslov, K.S. Grishakov, M.A. Gimaldinova, K.P.

- Katin, Carbon vs silicon polyprismanes: A comparative study of metallic sp³-hybridized allotropes. *Fuller. Nanotub. Car. Nanostructures* **28**, 97-103 (2020).
- [21] A.Y. Cao, P.L. Dickrell, W.G. Sawyer, M.N. Ghasemi-Nejhad, P.M. Ajayan, Super-compressible foamlike carbon nanotube films. *Science* **310**, 1307-1310 (2005).
- [22] L.K. Rysaeva, E.A. Korznikova, R.T. Murzaev, D.U. Abdullina, A.A. Kudreyko, J.A. Baimova, D.S. Lisovenko, S.V. Dmitriev, Elastic damper based on carbon nanotube bundle. *Facta Univ. Ser. Mech. Eng.* **18**, 1-12 (2020).
- [23] A. V. Savin, E. A. Korznikova, and S. V. Dmitriev, Scroll configurations of carbon nanoribbons. *Phys. Rev. B* **92**, 035412, (2015).
- [24] E.A. Korznikova, L.K. Rysaeva, A.V. Savin, E.G. Soboleva, E.G. Ekomasov, M.A. Ilgamov, S.V. Dmitriev, Chain model for carbon nanotube bundle under plane strain conditions. *Materials* **12**, 3951 (2019).
- [25] A. Savin, E. Korznikova, S. Dmitriev, and E. Soboleva, Graphene nanoribbon winding around carbon nanotube. *Comp. Mater. Sci.* **135**, 99-108 (2017).
- [26] A. V. Savin, E. A. Korznikova, and S. V. Dmitriev, Dynamics of surface graphene ripplocations on a flat graphite substrate. *Phys. Rev. B* **99**, 235411 (2019).
- [27] A. V. Savin and O. I. Savina, Bistability of Multiwalled Carbon Nanotubes Arranged on Plane Substrates. *Phys. Solid State* **61**, 2241 (2019).
- [28] J. Wang, F. Ma and M. Sun, Graphene, hexagonal boron nitride, and their heterostructures: properties and applications. *RSC Adv.* **7**, 16801 (2017).
- [29] C. Ling-Xiu, W. Hui-Shan, J. Cheng-Xin, C. Chen, W. Hao-Min, Synthesis and characterization of graphene nanoribbons on hexagonal boron nitride. *Acta Physica Sinica.* **68**(16), 168102 (2019).
- [30] G. Gao, T. Cagin, and W. A. Goddard III, Energetics, structure, mechanical and vibrational properties of single-walled carbon nanotubes. *Nanotechnology* **9**, 184 (1998).
- [31] J. Xiao, B. Liu, Y. Huang, J. Zuo, K.-C. Hwang, and M.-F. Yu, Collapse and stability of single- and multi-wall carbon nanotubes. *Nanotechnology* **18**, 395703 (2007).
- [32] J.A. Baimova, Q. Fan, L. Zeng, Z. Wang, S.V. Dmitriev, X. Feng, and K. Zhou, Atomic structure and energy distribution of collapsed carbon nanotubes of different chiralities. *J. Nanomater.* **2015**, 186231 (2015).
- [33] R. Fletcher, C.M. Reeves, Function Minimization by Conjugate Gradients. *Computer Journal*, **7**, 149-154 (1964).
- [34] L. Verlet, Computer "experiment" on classical fluids. I. Thermodynamical properties of Lennard-Jones molecules. *Phys. Rev.* **159**, 98-103 (1967).